

# Journal of Materials Chemistry A

Materials for energy and sustainability

Accepted Manuscript

This article can be cited before page numbers have been issued, to do this please use: A. Jegorove, X. Gao, P. Luizys, M. Daškeviien, S. Xing, R. Pau, J. Petrulevicius, V. Jankauskas, K. Rakstys, M. K. Nazeeruddin and V. Getautis, *J. Mater. Chem. A*, 2026, DOI: 10.1039/D5TA10419J.



This is an Accepted Manuscript, which has been through the Royal Society of Chemistry peer review process and has been accepted for publication.

Accepted Manuscripts are published online shortly after acceptance, before technical editing, formatting and proof reading. Using this free service, authors can make their results available to the community, in citable form, before we publish the edited article. We will replace this Accepted Manuscript with the edited and formatted Advance Article as soon as it is available.

You can find more information about Accepted Manuscripts in the [Information for Authors](#).

Please note that technical editing may introduce minor changes to the text and/or graphics, which may alter content. The journal's standard [Terms & Conditions](#) and the [Ethical guidelines](#) still apply. In no event shall the Royal Society of Chemistry be held responsible for any errors or omissions in this Accepted Manuscript or any consequences arising from the use of any information it contains.

# Facile design hydrazone-based Spiro-OMeTAD alternative hole transporting material for perovskite solar cells

View Article Online  
DOI: 10.1039/D5TA10419J

Aistė Jegorovė,<sup>a</sup> Xiao-Xin Gao,<sup>c\*</sup> Povilas Luizys,<sup>a</sup> Maryte Daskeviciene,<sup>a</sup> Shiyu Xing,<sup>c</sup> Riccardo Pau,<sup>c</sup> Julius Petrulevičius,<sup>a</sup> Vygintas Jankauskas,<sup>b</sup> Kasparas Rakstys,<sup>a</sup> Mohammad Khaja Nazeeruddin,<sup>c,d\*</sup> Vytautas Getautis<sup>a\*</sup>

<sup>a</sup>Department of Organic Chemistry, Kaunas University of Technology, Radvilėnų pl. 19, Kaunas, 50254 Lithuania

<sup>b</sup>Institute of Chemical Physics Vilnius University, Saulėtekio al. 3, Vilnius 10257, Lithuania

<sup>c</sup>Institute of Chemical Sciences and Engineering, École Polytechnique Fédérale de Lausanne (EPFL), CH 1015, Lausanne, Switzerland.

<sup>d</sup>Department of Mechanical and Energy Engineering, College of Engineering, Imam Abdulrahman Bin Faisal University, Dammam, P.O. Box 1982, 34212, Saudi Arabia

\*Corresponding authors: [xiaoxin.gao@epfl.ch](mailto:xiaoxin.gao@epfl.ch); [mdkhaja.nazeeruddin@epfl.ch](mailto:mdkhaja.nazeeruddin@epfl.ch); [vytautas.getautis@ktu.lt](mailto:vytautas.getautis@ktu.lt)

**Keywords:** hydrazone, perovskite solar cells, hole transporting material, Spiro-OMeTAD alternative

## ABSTRACT

Hydrazone-based hole-transporting material 9,9'-(hydrazine-1,2-diylidene)bis(*N*<sup>2</sup>,*N*<sup>2</sup>,*N*<sup>7</sup>,*N*<sup>7</sup>-tetrakis(4-methoxyphenyl)-9*H*-fluorene-2,7-diamine (**V1375**) has been synthesized using straightforward two-step procedure from commercially available and inexpensive starting reagents, mimicking synthetically challenging 9,9'-spirobifluorene moiety of well-studied Spiro-OMeTAD. The evaluated thermal properties reveal that pristine **V1375** exhibits a glass transition temperature of 132 °C and high thermal stability, with a 5 % mass loss occurring at 395 °C. Meanwhile, the measured intrinsic hole-transport mobility and conductivity reaches  $2.5 \cdot 10^{-6} \text{ cm}^2 \text{ V}^{-1} \text{ s}^{-1}$  and  $1.6 \cdot 10^{-4} \text{ S m}^{-1}$ , respectively. Power conversion efficiency over 24% with improved stability has been achieved by employing the doped **V1375** as a novel HTM in perovskite solar cells outperforming state-of-the-art Spiro-OMe-TAD.

## INTRODUCTION

Nowadays, environmental pollution is one of the world's biggest problems, causing ecological issues such as the greenhouse effect, droughts, floods, and increasing suffering caused by more frequent and



severe hurricanes and heat waves. These disasters lead to a shortages of food and water and disrupt the global food chain and biodiversity. Environmental contamination is primarily result of the usage of non-renewable energy resources, such as oil or coal; therefore, the utilization of clean and renewable energy sources is crucial. Over the past decade, renewable energy sources such as solar, wind, and geothermal power have achieved prominence, with their share of global energy generation now exceeding 10%.

Solar energy is one of the largest and most accessible energy sources available to humanity, leading to the invention of solar cells. Since the 1954,<sup>1</sup> solar technology has evolved significantly, resulting in the development of various types of solar cells. In 2009<sup>2</sup> the first publication on perovskite solar cells (PSCs) was released, sparking interest among scientists. Since then, intensive research has led to impressive efficiency improvements, with the highest performance recorded reaching 27 %.<sup>3</sup>

The perovskite material is particularly attractive for solar cell applications because of its long carrier diffusion length,<sup>4</sup> high absorption coefficient,<sup>5</sup> low exciton binding energy,<sup>6</sup> high charge carrier mobility,<sup>7</sup> and versatility in layer coating techniques.<sup>8</sup> However, several issues hinder the commercialization of PSCs, including poor perovskite material stability<sup>9</sup> and the high cost of commonly used hole-transporting materials (HTMs). Consequently, optimization of synthesis processes is required for developing cost-effective and stable devices.

While PSCs can generate electricity without a hole-transporting layer (HTL),<sup>10–12</sup> their efficiencies are typically higher when molecular organic HTMs are incorporated into n-i-p device structure. The highest performances have been achieved using 2,2',7,7'-tetrakis(*N,N*-di-*p*-methoxyphenylamine)-9,9'-spirobifluorene (Spiro-OMeTAD). However, the multi-step synthesis of Spiro-OMeTAD is excessively expensive since it includes reaction steps that require low temperature (-78 °C), sensitive (*n*-butyllithium or Grignard reagents) and aggressive (Br<sub>2</sub>) reagents. In addition, high-purity sublimation-grade Spiro-OMeTAD is required to obtain high-performance devices. Even after synthesis optimization, this material still requires four synthesis steps.<sup>13</sup>

For this reason, scientists have focused their attention on finding new HTMs that can be synthesized through simple methods while exhibiting desirable properties. Consequently, numerous new materials, including compounds of spirobifluorene,<sup>14–16</sup> fluorene,<sup>17–19</sup> fluorenylidene,<sup>20–22</sup> and carbazole,<sup>23–25</sup> have been proposed as HTMs for efficient device fabrication. Meanwhile, hydrazones, a well-known, easily synthesised class of materials, are not widely used as hole-transporting materials in PSCs. However, over the past decade, they have been among the most popular families of materials used for electrophotographic photoreceptors.<sup>26–28</sup> To the best of our knowledge, only a few publications investigated the application of hydrazones as HTMs for perovskite solar cells.<sup>29–32</sup>



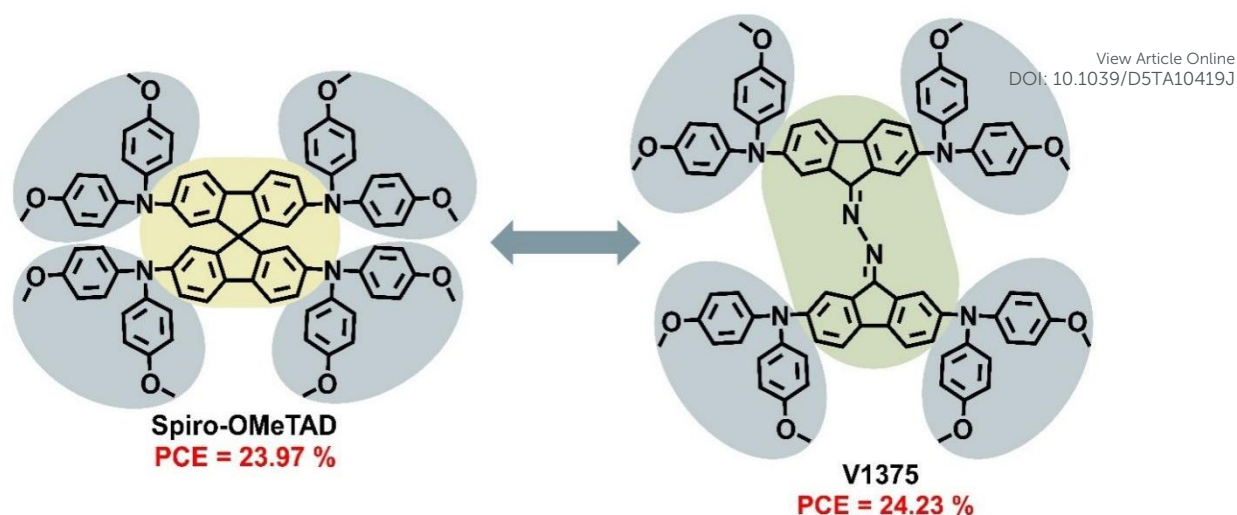
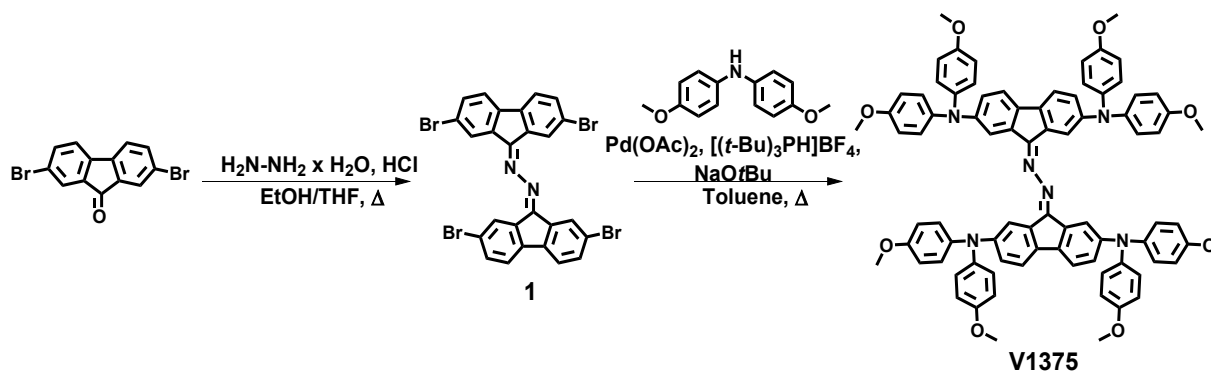


**Figure 1.** Chemical structures of Spiro-OMeTAD and hydrazone-based **V1375**

In this manuscript we describe hydrazone-based material **V1375**, which was synthesized via simple two-step synthesis strategy and used in an n-i-p device configuration (Figure 1). The power conversion efficiency of perovskite solar cells using **V1375** reaches 24.23%, which is very similar to that achieved with Spiro-OMeTAD (23.97%). Moreover, the long-term stability of the champion solar cell was greater than that of devices using Spiro-OMeTAD.

## RESULTS AND DISCUSSIONS

Hydrazone-based HTM was synthesized using Buchwald-Hartwig reaction conditions using 4,4'-dimethoxydiphenylamine as a side fragment. As shown in Scheme 1, in the first step, the corresponding central hydrazone-bridged bifluorene fragment was produced from 2,7-dibromofluoren-9-one via a hydrazone condensation reaction, yielding intermediate **1**, which was filtered after the reaction, washed with hot acetone, and afterwards treated with 4,4'-dimethoxydiphenylamine in the presence of palladium catalyst to obtain target material **V1375**. The chemical structure of target material was confirmed by NMR spectroscopy and mass spectrometry. Detailed description of the synthetic procedures is provided in the Supporting Information.



**Scheme 1.** Synthetic route to intermediate **1** and target compound **V1375**.



Considering the simple syntheses of **V1375**, its material costs were assessed based on the model described by Dingemans, Docampo, and Osedach,<sup>33</sup> which is about 29.58 \$/g (Table S1). It would cost three times less to produce this HTM than widely used standard Spiro-OMeTAD, which costs 92 \$/g to synthesize.

To determine the conjugation of the new compound, UV-vis absorption spectra of THF solution ( $c = 10^{-4}$  M) were recorded (Figure 3a). **V1375** exhibits four absorption peaks. The absorption spectrum of **V1375** is slightly redshifted compared to that of Spiro-OMeTAD, indicating negligible enhancement of  $\pi$ -conjugation. The peaks in the range of 230–425 nm can be assigned to  $\pi \rightarrow \pi^*$  transitions, while a barely noticeable absorption band in the visible region at 544 nm is a result of  $\pi \rightarrow \pi^*$  transitions with charge transfer character, which arises because of electron-rich hydrazone units. This is also in good agreement with the density functional theory (DFT) calculations, performed at the B3LYP/6-31G(d,p) level of theory, where the highest occupied molecular orbital (HOMO) of the **V1375** molecule is mainly distributed over the dimethoxy diphenylamine substituted fluorene fragments. Upon excitation, the lowest unoccupied molecular orbital (LUMO) is highly delocalized over the hydrazone units (Figure 2).

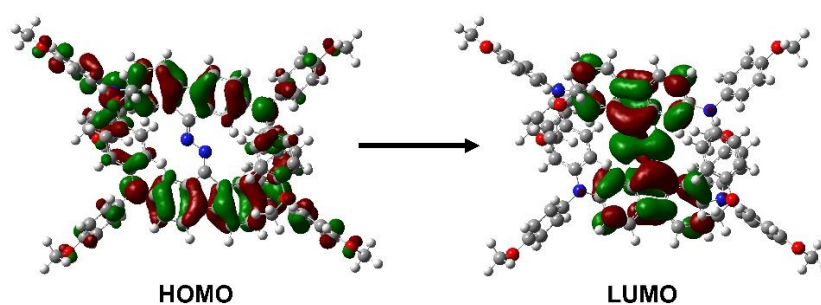


**Figure 2.** Frontier Kohn–Sham molecular orbitals of **V1375** were obtained from theoretical calculations at the B3LYP/6-31G(d,p) level of theory.

The thermal properties of **V1375** were evaluated using thermogravimetric analysis (TGA) and differential scanning calorimetry (DSC). The results are presented in Table 1 and Figure 3b,c. From TGA data, it was found that hydrazone-based HTM demonstrates a relatively high decomposition temperature ( $T_{d5}$ ) of 395 °C at 5 % weight loss, which is similar to that of spiro-OMeTAD (413 °C), indicating good thermal stability required for photovoltaic device.<sup>34</sup> The DSC analysis revealed that **V1375** exhibited one endothermic peak, appearing at around 300 °C, is typically associated with a melting process. No crystallization was observed during the cooling and second heating steps, only the glass transition ( $T_g$ ) at 132 °C, which is comparable to the  $T_g$  of Spiro-OMeTAD, suggesting that the material could exist in both crystalline and amorphous states. Moreover, we have evaluated  $T_g$  of **V1375** upon mixing it with the additives that are typically employed in the fabrication of PSC. As shown in Fig. S6, upon doping **V1375** possesses a significantly lower  $T_g$  value comparing to undoped



value (132 °C), which may be caused by the migration and volatilization of dopants at high temperature.<sup>35</sup> We next evaluated  $T_g$  of doped Spiro-OMeTAD and it was found that upon doping Spiro-OMeTAD suffers a significant drop in  $T_g$  possessing even lower  $T_g$  value of 67 °C compared to doped **V1375**, therefore, while doped **V1375**  $T_g$  is 78 °C, it is still demonstrating superior thermal stability at 65 °C in operando compared to the reference (Figure S7).

The energy level of **V1375** was estimated by photoelectron spectroscopy in air (PESA), yielding an ionization potential ( $I_P$ ) of 4.92 eV (see Table 1 and Figure 3d). Compared with Spiro-OMeTAD ( $I_P$  = 4.91 eV), it is evident that presence of hydrazone group in the center of molecule does not change the  $I_P$ , suggesting that the synthesized compound would be suitable for use in PSCs.

The hole drift mobility ( $\mu_0$ ) was measured using xerographic time-of-flight (XTOF) method, and the results are presented in Table 1 and Figure 3e. The data show that **V1375** exhibits a hole drift mobility of  $2.5 \cdot 10^{-6} \text{ cm}^2 \text{ V}^{-1} \text{ s}^{-1}$  at zero electric field strength, which is lower than that of Spiro-OMeTAD ( $\mu_0 = 1.4 \cdot 10^{-5} \text{ cm}^2 \text{ V}^{-1} \text{ s}^{-1}$ ). This difference can be attributed to the flexible backbone of the hydrazone-based material, which may induce conformational and energetic disorder, thereby reducing hole drift mobility. The intrinsic conductivity ( $\sigma$ ) was evaluated using current measurement (Figure 3f) and it was found that **V1375** has 2.5 times higher conductivity than Spiro-OMeTAD,  $1.6 \cdot 10^{-4}$  and  $6.4 \cdot 10^{-5} \text{ S m}^{-1}$ , respectively, attributing to the higher concentration of holes in the **V1375** material.

**Table 1.** Thermal, optical and photophysical properties of **V1375** and Spiro-OMeTAD.

HTM	$T_g$ [°C] <sup>a)</sup>	$T_m$ [°C] <sup>a)</sup>	$T_{d5}$ [°C] <sup>a)</sup>	$\lambda_{\text{abs}}$ [nm] <sup>b)</sup>	$I_P$ [eV] <sup>c)</sup>	$\mu_0$ [cm <sup>2</sup> V <sup>-1</sup> s <sup>-1</sup> ] <sup>d)</sup>	$\sigma$ [S m <sup>-1</sup> ]
<b>V1375</b>	132	303	395	297, 339, 383, 544	4.92	$2.5 \cdot 10^{-6}$	$1.6 \cdot 10^{-4}$
<b>Spiro-OMeTAD</b>	138	249	413	237, 303, 367, 387	4.91	$1.4 \cdot 10^{-5}$	$6.4 \cdot 10^{-5}$

<sup>a)</sup>Glass transition ( $T_g$ ), melting point ( $T_m$ ) and 5% weight loss ( $T_{d5}$ ) temperatures observed from DSC and TGA measurements, respectively (10 °C min<sup>-1</sup>, N<sub>2</sub> atmosphere); <sup>b)</sup>UV-vis spectra measured in tetrahydrofuran (THF) solutions (10<sup>-4</sup> M); <sup>c)</sup>Ionization energies of the films measured using PESA; <sup>d)</sup>Mobility value at zero field strength.



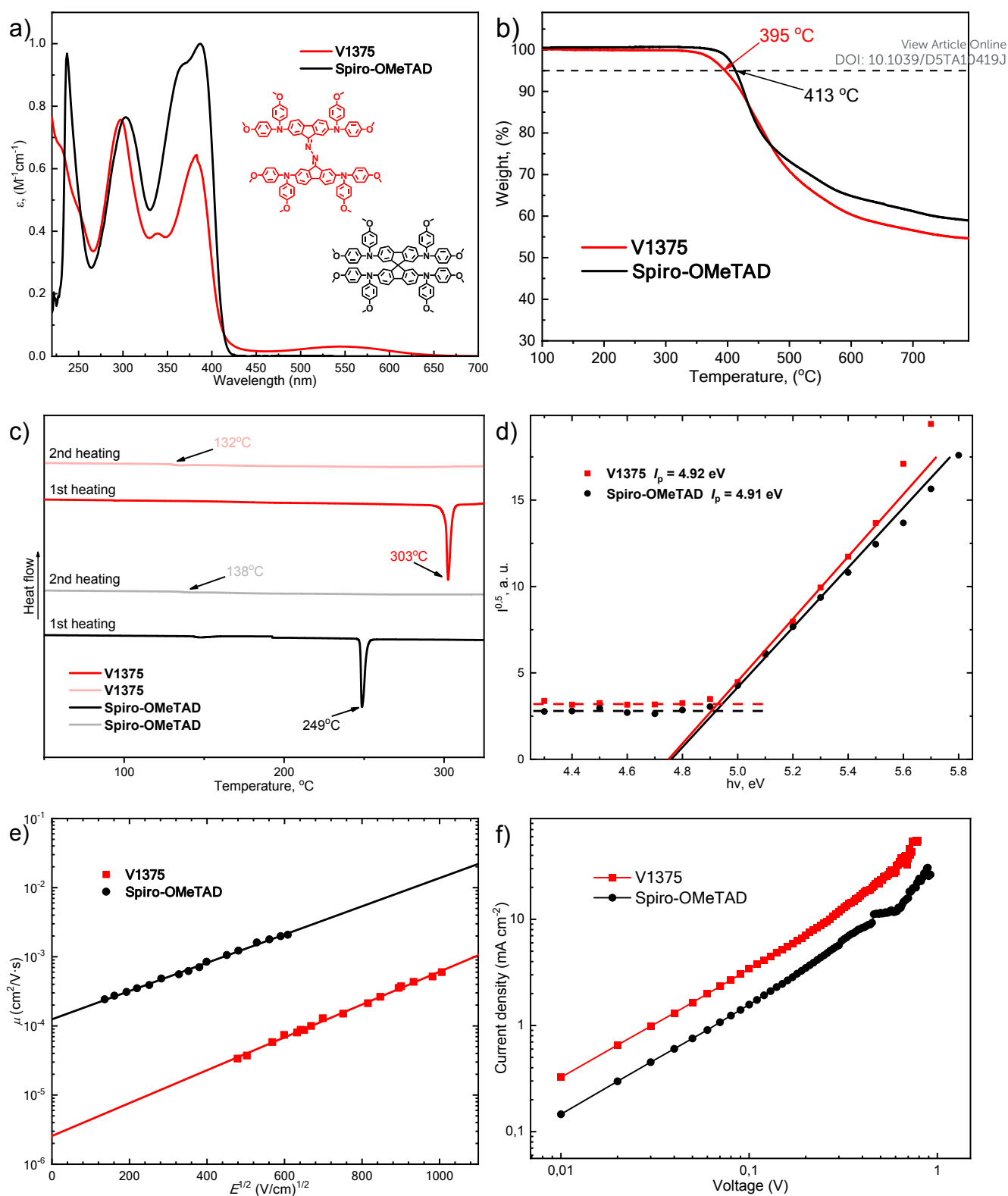


**Figure 3.** a) Normalized UV-vis absorption spectra of **V1375** and Spiro-OMeTAD from THF solutions ( $10^{-4}$  M); b) TGA heating curve of **V1375** and Spiro-OMeTAD (heating rate of  $10\text{ }^{\circ}\text{C min}^{-1}$ ,  $\text{N}_2$  atmosphere); c) DSC curve of the first heating of **V1375** and Spiro-OMeTAD; d) Ionization potential of **V1375** and Spiro-OMeTAD; e) Hole drift mobility of target material **V1375** and Spiro-OMeTAD; f) Conductivity of target material **V1375** and Spiro-OMeTAD.



The performance of the constructed devices is summarized in Table 2. Figure 4a,b presents the  $J-V$  curves of the champion PSCs. The highest PCE of the reference (Spiro-OMeTAD) device was 23.97%, whereas **V1375**-based device achieved 24.23%. The best-performing device of **V1375** exhibited a  $V_{OC}$  of 1.119 V,  $J_{SC}$  of 26.12 mA/cm<sup>2</sup>, and a fill factor (FF) of 0.825. Additionally, the hysteresis indices (HI) were evaluated for both the reference and **V1375** devices (Figure 4a,b), revealing that the latter exhibits lower HI values. The EQE spectra and statistics of the photovoltaic parameters are shown in **Figures S4-S5**.

**Table 2.** PV characteristics derived from the corresponding  $J-V$  curves of the best-performing devices.

HTM	$V_{oc}$ [V]	$J_{sc}$ [mA/cm <sup>2</sup> ]	FF	PCE [%]
<b>V1375</b>	1.119	26.12	0.825	24.23
<b>Spiro-OMeTAD</b>	1.113	26.09	0.822	23.97

The long-term stability of the PSCs was evaluated under maximum power point (MPP) tracking conditions for 950 hours in an inert environment (Figure 4c). After this period, the reference device retained only 65% of its initial efficiency, whereas devices employing **V1375** as the HTM exhibited improved stability, maintaining 85% of their original efficiency. Additional MPP decay measurements were conducted at 65 °C. All PSCs were tested in an N<sub>2</sub> atmosphere under continuous illumination of 100 mW cm<sup>-2</sup>. As shown in Figure 4d, the device incorporating **V1375** as the HTM exhibited superior thermal stability compared to the untreated reference device. After 500 hours of continuous light soaking, the **V1375**-based device retained 89 % of its initial MPP value, whereas the reference devices maintained only 75%.



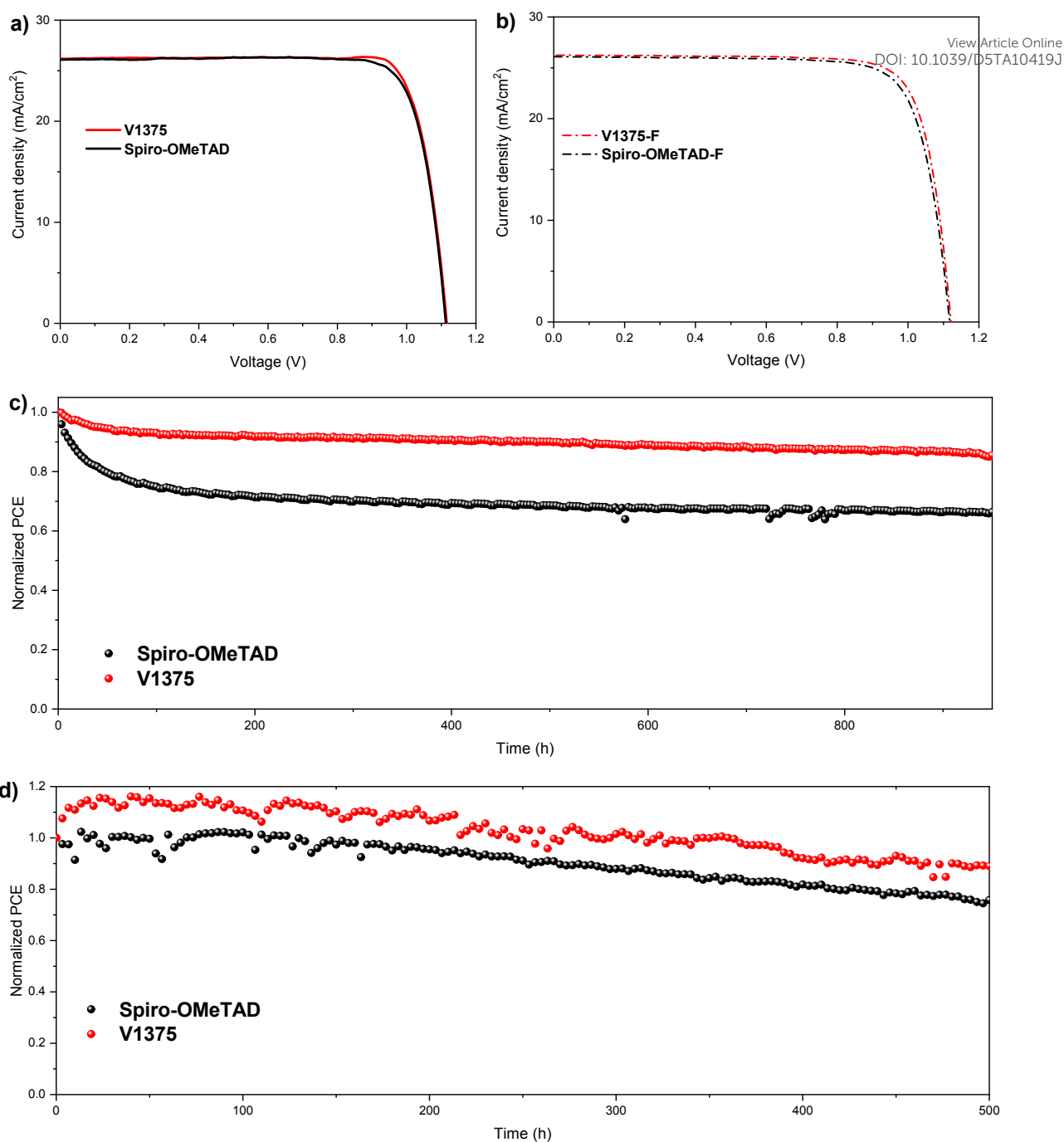


**Figure 4.** a)  $J-V$  reverse scan (RS) curves and b)  $J-V$  forward scan (FS) curves of the perovskite champion devices with V1375 and reference devices recorded under one sun illumination; c) Light-induced stability of perovskite devices incorporating V1375 and reference materials. The devices were measured in a N<sub>2</sub> atmosphere at room temperature, under constant illumination (LED source,  $\approx 1$  Sun) at the maximum power point for 950 h; d) Thermal stability of perovskite devices incorporating V1375 and reference materials. The devices were measured in a N<sub>2</sub> atmosphere at 65 °C, under continuous illumination (LED source,  $\approx 1$  Sun) at a maximum power point for 500 h.



## CONCLUSION

In this study, a hydrazone-based HTM **V1375**, containing 4,4'-dimethoxydiphenylamine chromophores, was synthesized and evaluated as potential replacement for Spiro-OMeTAD in perovskite solar cells. **V1375** exhibits high thermal stability and a relatively high glass transition temperature. Perovskite solar cells incorporating **V1375** achieved a maximum efficiency of 24.23 %, outperforming the benchmark Spiro-OMeTAD (23.97 %). The simplicity of a cost-effective and upscalable synthesis should enable rapid advancement of this material for perovskite solar cells and other optoelectronic applications.

## ACKNOWLEDGEMENTS

This project is co-funded by the European Union. Views and opinions expressed are however those of the author(s) only and do not necessarily reflect those of the European Union or the European Climate, Infrastructure and Environment Executive Agency (CINEA). Neither the European Union or the granting authority can be held responsible for them. PEPPERONI, ID: 101084251. We acknowledge the funding from project “Mission-driven Implementation of Science and Innovation Programmes” (No. 02-002-P-0001), funded by the Economic Revitalization and Resilience Enhancement Plan “New Generation Lithuania”.

## AUTHOR CONTRIBUTION

A.J. and P.L. performed the synthesis and wrote the first manuscript draft. X.-X.G. designed the experiments and fabricated PSCs. M.D. and J.P. contributed to DFT calculations and molecular dynamics simulations. S.X. and R.P. helped with the device fabrication and characterization. V.J. performed hole mobility measurements. K.R. was involved in discussion and project coordination. M.K.N. and V.G. supervised the project. All the authors contributed to the revisions.

## REFERENCES

1. D. M. Chapin, C. S. Fuller, and G. L. Pearson. *Journal of Applied Physics* **1954**, 25 (5), 676–677.
2. A. Kojima, K. Teshima, Y. Shirai, and T. Miyasaka. *J. Am. Chem. Soc.* **2009**, 131, 17, 6050–6051.
3. <https://www.nrel.gov/pv/cell-efficiency.html>. (accessed: October 2025)
4. Q. Dong, Y. Fang, Y. Shao, P. Mulligan, J. Qiu, L. Cao, and J. Huang. *Science* **2014**, 347, 6225, 967–970.
5. W. J. Yin, T. Shi, Y. Yan. *Adv. Mater.* **2014**, 26, 4653–4658.



6. A. Miyata, A. Mitioglu, P. Plochocka, O. Portugall, J. T. W. Wang, S. D. Stranks, H. J. Snaith, and R. J. Nicholas. *Nature Phys* **2015**, 11, 582–587.

View Article Online  
DOI: 10.1039/D5TA10419J

7. C. Wehrenfennig, G. E. Eperon, M. B. Johnston, H. J. Snaith, L. M. Herz. *Adv. Mater.* **2014**, 26, 1584–1589.

8. N. K. Elangovan, R. Kannadasan, B. B. Beenarani, M. H. Alsharif, M. K. Kim, Z. H. Inamul. *Energy Reports* **2024**, 11, 1171–1190.

9. H. Miah, B. Rahman, M. Nur-E-Alam, M. A. Islam, M. Shahinuzzaman, R. Rahman, H. Ullahi, and M. Khandaker. *RSC Adv.* **2025**, 15, 628–654.

10. R. R. Sova, Shobih, W. Budiawan, W. Septina, L. Yuliantini, Y. Firdaus, E. Almuqoddas, B. Yulianto, N. M. Nursam. *Synthetic Metals* **2024**, 306, 117646.

11. W. Passatorntaschakorn, W. Khampa, W. Musikpan, A. Ngamjarurojana, A. Gardchareon, P. Kanjanaboos, A. Kaewprajak, P. Kumnorkaew, P. Ruankham, D. Wongratanaphisan. *ACS Appl. Energy Mater.* **2024**, 7, 16, 6972–6985.

12. G. Huang, T. Zhang, W. Lin, L. Qin, S. Z. Kang, and X. Li. *Angew. Chem. Int. Ed.* **2025**, 64, e202420687.

13. S. Mattiello, G. Lucarelli, A. Calascibetta, L. Polastri, E. Ghiglietti, S. K. Podapangi, T. M. Brown, M. Sassi, and L. Beverina. *ACS Sustainable Chem. Eng.* **2022**, 10, 14, 4750–4757.

14. Y. Ren, Y. Wei, T. Li, Y. Mu, M. Zhang, Y. Yuan, J. Zhanga, and P. Wang. *Energy Environ. Sci.*, **2023**, 16, 3534–3542.

15. X. Wang, M. Wang, Z. Zhang, D. Wei, S. Cai, Y. Li, R. Zhang, L. Zhang, R. Zhang, C. Zhu, X. Huang, F. Gao, P. Gao, Y. Wang, and W. Huang. *Research* **2024**, 7, 0332.

16. Y. Luo, T. Li, L. He, L. Dong, T. Xie, Y. Ren, Z. Zhang, G. Yang, Y. Jia, J. Zhou, K. Guo. *Adv. Funct. Mater.* **2025**, 35, 2419849.

17. R. Li, M. Liu, S. K. Matta, A. Almasri, J. Tian, H. Wang, H. P. Pasanen, S. P. Russo, P. Vivo, H. Zhang. *Sol. RRL* **2023**, 7, 2300367.

18. P. Mäkinen, F. Fasulo, M. Liu, G. K. Grandhi D. Conelli, B. Al-Anesi, H. Ali-Löyty, K. Lahtonen, S. Toikkonen, G. P. Suranna, A. B. Muñoz-García, M. Pavone, and R. Grisorio. *Chem. Mater.* **2023**, 35, 7, 2975–2987.

19. C. Hao, X. Zong, Y. Cheng, M. Zhao, M. Luo, Y. Zhanga, and S. Xue. *Sustainable Energy Fuels* **2021**, 5, 5548–5556.

20. A. Jegorovė, J. Xia, M. Steponaitis, M. Daskeviciene, V. Jankauskas, A. Gruodis, E. Kamarauskas, T. Malinauskas, K. Rakstys, K. A. Alamry, V. Getautis, M. K. Nazeeruddin. *Chem. Mater.* **2023**, 35, 15, 5914–5923.



21. B. Xiao, Y. Yang, S. Chen, Y. Zou, X. Chen, K. Liu, N. Wang, Y. Qiao, X. Yin. *Sol. RRL* **2022**, 6, 2100990. View Article Online  
DOI: 10.1039/D5TA10419J
22. S. C. Lin, T. H. Cheng, C. P. Chen, Y. C. Chen. *Materials Chemistry and Physics* **2022**, 288, 126385.
23. A. A. Sutanto, V. Joseph, C. Igci, O. A. Syzgantseva, M. A. Syzgantseva, V. Jankauskas, K. Rakstys, V. I. E. Queloz, P. Y. Huang, J. S. Ni, S. Kinge, A. M. Asiri, M. C. Chen, M. K. Nazeeruddin. *Chem. Mater.* **2021**, 33, 9, 3286–3296
24. H. Liu, B. He, H. Lu, R. Tang, F. Wu, C. Zhong, S. Li, J. Wang, and L. Zhu. *Sustainable Energy Fuels*, **2022**, 6, 371–376.
25. Y. J. Kim, B. Yang, J. Suo, E. Jatautiene, J. Simokaitiene, R. Durgaryan, D. Volyniuk, A. Hagfeldt, G. Sini, J. V. Grazulevicius. *Nano Energy*, **2022**, 101, 107618.
26. J. Simokaitiene, A. Danilevicius, S. Grigalevicius, J. V. Grazulevicius, V. Getautis, V. Jankauskas, *Synthetic Metals*, **2006**, 156, 14–15, 926–931.
27. R. Budreckiene, J. V. Grazulevicius, V. Jankauskas, J. Vedegyte, J. Sidaravicius. *Journal of optoelectronics and advanced materials*, **2006**, 8, 4, 1533–1537.
28. R. Budreckiene, V. Andruleviciute, G. Buika, J. V. Grazulevicius, V. Jankauskas, V. Grazuleviciene. *Materials Science-Poland*, **2009**, 27, 1, 61–72.
29. M. L. Petrus, M. T. Sirtl, A. C. Closs, T. Bein, and P. Docampo. *Mol. Syst. Des. Eng.*, **2018**, 3, 734–740.
30. M. L. Petrus, A. Music, A. C. Closs, J. C. Bijleveld, M. T. Sirtl, Y. Hu, T. J. Dingemans, T. Bein, and P. Docampo. *J. Mater. Chem. A*, **2017**, 5, 25200–25210.
31. C. Decavoli, C. L. Boldrini, A. Abbotto, N. Manfredi. *Eur. J. Org. Chem.* **2023**, 26, e202201511.
32. R. Durgaryan, J. Simokaitiene, A. Dabuliene, D. Volyniuk, O. Bezikonny, V. Jankauskas, V. Matulis, D. Lyakhov, I. Klymenko, B. Schmaltz, and J. V. Grazulevicius. *Synthetic Metals*, **2022**, 287, 117057.
33. T. P. Osedach, T. L. Andrew and V. Bulovic. *Energy Environ. Sci.*, **2013**, 6, 711–718.
34. R. Gehlhaar, T. Merckx, W. Qiu, and T. Aernouts. *Global Challenges*, **2018**, 2, 1800008.
35. X. Wang, Y. Zhong, Y. Liu, X. Luo, B. Gao, L. Tan, and Y. Chen. *Angew. Chem. Int. Ed.*, **2025**, 64, e202424191.



### DATA AVAILABILITY STATEMENT

The data that supports the findings of this study are available within the article and its supplementary material. Additional data will be available online under repository link once the article will be accepted for publication, or from the corresponding author upon request.

We note that there are not any restrictions on data availability (e.g., proprietary data, privacy concerns). Sincerely yours,

Vytautas Getautis

